



Regular article

Selective phase formation in substoichiometric Al-Cr-based oxides

C.M. Koller^{a,b,*}, V. Dalbauer^a, A. Kirnbauer^b, S. Löffler^c, S. Kolozsvári^d, J. Ramm^e, P.H. Mayrhofer^{a,b}^a Christian Doppler Laboratory for Application Oriented Coating Development at the Institute of Materials Science and Technology, TU Wien, Vienna, Austria^b Institute of Materials Science and Technology, TU Wien, Vienna, Austria^c Universitäre Service-Einrichtung für Transmissionselektronenmikroskopie, TU Wien, Vienna, Austria^d Plansee Composite Materials GmbH, Lechbruck am See, Germany^e Oerlikon Balzers, Oerlikon Surface Solutions AG, Balzers, Liechtenstein

ARTICLE INFO

Article history:

Received 15 May 2017

Received in revised form 19 June 2017

Accepted 21 June 2017

Available online xxxxx

Keywords:

PVD, (Al,Cr)₂O₃

Intermetallic Al-Cr

Nano-composite

Transmission electron microscopy

ABSTRACT

The transition from (inter)metallic to substoichiometric regime and therewith associated microstructural modifications within arc evaporated Al-Cr-based oxide coatings was investigated. The dense columnar intermetallic structure is subject to grain refinement when increasing the O₂ flow rate during the deposition. Cr-rich, O-depleted crystalline domains (initially short columnar, then equiaxed globular) and an amorphous Al- and O-enriched boundary phase develops—with increasing volume fraction for higher O₂ flow rates. Such nanocomposites, originating from preferred oxide phase formation of Aluminium, can effectively be adjusted by the amount of oxygen and the nominal cathode composition used during synthesis.

© 2016 Acta Materialia Inc. Published by Elsevier Ltd. All rights reserved.

Al₂O₃ and Al₂O₃-based hard coatings prepared by physical vapour deposition (PVD) bear great potential for applications, which require high temperature stability, mechanical strength, and resistance in oxidative and corrosive environments. A major aim within the last years was the reduction of the synthesis temperature in order to widen the range of accessible substrates. Growth temperatures of >800 °C, which are typically used to prepare corundum (α) Al₂O₃ by chemical vapour deposition [1], lie beyond the maximum heat input many substrates can tolerate. However, elevated temperatures are necessary to promote the growth of dense films, consisting of the thermodynamically stable corundum structure. For PVD in general, and cathodic arc evaporation in particular, the addition of Cr as substituent for Al can effectively stabilise α-structured (Al_{1-x}Cr_x)₂O₃ solid solutions already at 500–600 °C [2]. However, the phase composition strongly correlates with the Cr content and single-phase corundum-type coatings are only realised for x ≥ 0.5. For higher Al contents, the frequently observed metastable Al-Cr-O phases within PVD coatings [3–5] transform into α-(Al_{1-x}Cr_x)₂O₃ between 900 and 1050 °C [6]. The pronounced ionic bonding character of Al₂O₃ [7] (and therefore also of Al-rich (Al_{1-x}Cr_x)₂O₃-based coatings) is responsible for the sensitivity to deposition (e.g., oxygen atoms available to react with metallic species) as well as nucleation and growth conditions present [8–10]. Crystalline seed layers like α-Cr₂O₃ can be used to trigger the nucleation of α-Al₂O₃ or α-(Al_{1-x}Cr_x)₂O₃ [11,12]. A

similar mechanism was recently also associated with specific three-dimensional defects (i.e., macroparticles) [13].

In the present study, we aim for a more in-depth understanding of the phase formation during growth of Al-Cr-based oxides and how the coating microstructure is affected in the regime of deficient reactive gas flow placing emphasis on the formation of substoichiometric material of nano-sized structures.

All coatings investigated were synthesised in an Oerlikon Balzers Innova arc evaporation facility using powder-metallurgically produced Al_{0.75}Cr_{0.25}, Al_{0.70}Cr_{0.30}, Al_{0.50}Cr_{0.50}, and Al_{0.25}Cr_{0.75} cathodes (6 in with 99.9% purity, Plansee Composite Materials GmbH). Si (100) substrates were ultrasonically cleaned in ethanol and acetone for 15 min and placed onto a two-fold substrate rotation holder (minimum substrate-to-cathode distance ~25 cm). The deposition chamber was heated to 450 °C and prior to the deposition an Ar-ion etching procedure was conducted for 30 min. The arc was operated at 180 A (symmetrical arrangement of 4 cathodes) and the substrates were bipolar pulsed with –60 V. Oxygen was flow-controlled introduced to the cathodes by either 50 or 100 sccm per active source (p.a.s.), which guaranteed for films with an average oxygen content below 60 at.% (present in sesquioxides). The total deposition time was 45 min. A second set of coatings, containing an oxygen gradient along the cross-section, was established by increasing the oxygen flow rate from 0 to 250 sccm p.a.s. throughout the 76 min lasting deposition. The evaporation rate depends strongly on oxygen flow under these conditions and therefore an Fe-containing layer (by the ignition of two additional Al_{0.675}Cr_{0.275}Fe_{0.05} cathodes) was grown after each 25 sccm O₂ step, which was used as tracer being able separating the different flow regimes and their corresponding

* Corresponding author at: Institute of Materials Science and Technology, TU Wien, Vienna, Austria.

E-mail address: christian.martin.koller@tuwien.ac.at (C.M. Koller).

microstructural features by subsequent chemical analyses. A FEI Tecnai F20 transmission electron microscope (TEM) with a field emission gun operated at 200 keV was used for structural investigations. Chemical analyses were carried out in scanning mode (STEM) using energy dispersive X-ray spectroscopy (EDS) and electron energy loss spectroscopy (EELS). Samples were cross-sectionally prepared by mechanical grinding and a subsequent ion polishing procedure.

The Al and Cr contents of substoichiometric Al–Cr-based oxides deviate from the nominal cathode composition depending on oxygen flow rate and cathode composition. Generally, lower oxygen flow rates and higher Cr contents result in a lower Al/Cr-ratio. Coatings prepared from $\text{Al}_{0.70}\text{Cr}_{0.30}$ cathodes with 50 and 100 sccm O_2 p.a.s., for instance, exhibit an average chemical composition of 50 at.% Al, 25 at.% Cr, 25 at.% O, and 35 at.% Al, 15 at.% Cr, 50 at.% O, respectively. For easier reading, we will nonetheless refer to our coatings by the cathode composition used, e.g., $\text{Al}_{0.70}\text{Cr}_{0.30}$ -based coating.

The substoichiometric $\text{Al}_{0.70}\text{Cr}_{0.30}$ -based film grown with 50 sccm O_2 p.a.s. consists of a dual-phase microstructure of globular crystallites which are surrounded by a featureless boundary phase. The latter appears bright in the TEM BF studies, Fig. 1a and b, respectively. The average crystallite size is between 10 and 60 nm. Selected area electron diffraction (SAED) indicates fine-grained polycrystalline $\gamma_2\text{-Al}_8\text{Cr}_5$ (ICDD #00-029-0015), which is in good agreement with complementary XRD studies (not shown). No Al_2O_3 phase or any other crystalline oxide structure can be detected. The high-resolution image, Fig. 1b, highlights the crystalline nature of the dark globular areas and the Fast Fourier Transformation (FFT) corroborates a $\gamma_2\text{-Al}_8\text{Cr}_5$ structure (see inset), whereas the surrounding areas do not exhibit crystallinity.

In the subsequent discussion we refer to such areas without distinct/detectable lattice planes/arrangements as amorphous.

The coating prepared from $\text{Al}_{0.70}\text{Cr}_{0.30}$ cathodes with 100 sccm O_2 p.a.s. shown in Fig. 1c demonstrates a slightly different microstructure, consisting of layered crystalline features. Throughout the entire coating a more or less pronounced repetition of one broad and three thinner layers is visible. SAED carried out at an intermediate position shows one continuous diffraction ring ($d \approx 2.09\text{--}2.12 \text{ \AA}$) next to a bright background. This significant change in the diffraction pattern results from a further refinement of the crystalline areas (or distortion of crystalline growth) due to the higher fraction of incorporated oxygen.

The strongest diffraction peak for a γ -type Al_2O_3 should be detectable at $d \approx 1.98 \text{ \AA}$, and also the recently reported face-centred cubic B1-like $(\text{Al,Cr})_2\text{O}_3$ solid solution [5,14] would exhibit high intensity peaks at $d \approx 1.99 \text{ \AA}$, both of which are missing in the SAED pattern. However, intermetallic AlCr_2 (ICDD #03-065-2640) or $\gamma_2\text{-Al}_8\text{Cr}_5$ exhibit their strongest peaks for $d \approx 2.12 \pm 0.2 \text{ \AA}$, thus in good agreement with actual electron diffraction pattern and X-ray diffraction studies (not shown). Higher magnification images (exemplarily shown in Fig. 1d) reveal crystalline regions with lattice plane distances of 2.12 \AA , basically confirming SAED. For some regions, however, a lattice plane distance of 1.98 \AA is given and one can speculate whether small-sized metallic Cr ($\sim 2.03\text{--}2.04 \text{ \AA}$, ICDD #00-006-0694), a Cr(Al) solid solution, or even metastable cubic-structured $(\text{Al,Cr})_2\text{O}_3$ phases (e.g., θ - or $\gamma\text{-Al}_2\text{O}_3$) next to the dominating randomly oriented $\gamma_2\text{-Al}_8\text{Cr}_5$ crystallites are present.

A layered appearance similar to that in Fig. 1c is not an uncommon observation in arc evaporated coatings, which were grown by the use of a rotating substrate holder (examples are provided in the appendix). For coatings processed in oxygen-rich conditions, these structures typically appear after nucleation at the very beginning of film growth—which is dominated by competitive growth and small crystallite sizes—or during re-nucleation on macroparticles. Moreover, the alloying of $\text{Al}_{0.70}\text{Cr}_{0.30}$ -based coatings with certain elements also favours the formation of recurrent structures, although a regular cathode arrangement of 4 identical compound cathodes was chosen. In the case of $(\text{Al}_{0.70}\text{Cr}_{0.30})_2\text{O}_3$ coatings alloyed with Ta (not yet published) we found that the addition of up to 10 at.% Ta gradually promotes the formation of layered, chemically different features. However, also Al-rich films exhibit pronounced structural features under certain growth conditions as can be seen in Fig. 1d, showing the $\text{Al}_{0.70}\text{Cr}_{0.30}$ -based coating prepared with 100 sccm O_2 p.a.s. The EDS line scan carried out in growth direction across these layered structures shows an increase in Cr (blue line) for the bright contrasted areas whilst the Al (red line) and—more pronounced—O (green line) contents decrease. The repetition of 1 thick and 3 thinner layers is due to the cathode arrangement and geometric setup and speed of the two-fold rotating substrate holder in our facility. These structural and chemical alternations are in excellent agreement with observations made for a various number of sub- and stoichiometric $(\text{Al,Cr})_2\text{O}_3$ coatings (see the supplementary material), although the visible differences are not as pronounced as here. We therefore conclude that similar to the observations made for $(\text{Ti,Al})(\text{O,N})$ coatings [15], certain substrate positions in relation to the plasma flux lead to different reactivities of the species involved, resulting in these layered features. These structural and chemical separations (likely also affected by plasma density differences) are more pronounced for higher mass- and reactivity-differences between Al and the additional alloying element. Furthermore, such unintended layered elemental variations in $(\text{Al,Cr})_2\text{O}_3$ and $(\text{Al,Cr,M})_2\text{O}_3$ (e.g., $M = \text{Ta}$) films are more pronounced in the initial growth and re-nucleation regions (e.g., on large droplets), where competitive growth is dominant (see supplementary).

Detailed studies of the microstructural evolution of Al–Cr-based oxides from metallic to the stoichiometric oxide regime are conducted on coatings prepared with gradually increasing oxygen flow rate (from 0 to 250 sccm O_2 p.a.s.) during the deposition. These studies are conducted for $\text{Al}_{0.75}\text{Cr}_{0.25}$ -, $\text{Al}_{0.70}\text{Cr}_{0.30}$ -, $\text{Al}_{0.50}\text{Cr}_{0.50}$ -, $\text{Al}_{0.25}\text{Cr}_{0.75}$ -based coatings to investigate and identify the essential chemical and structural

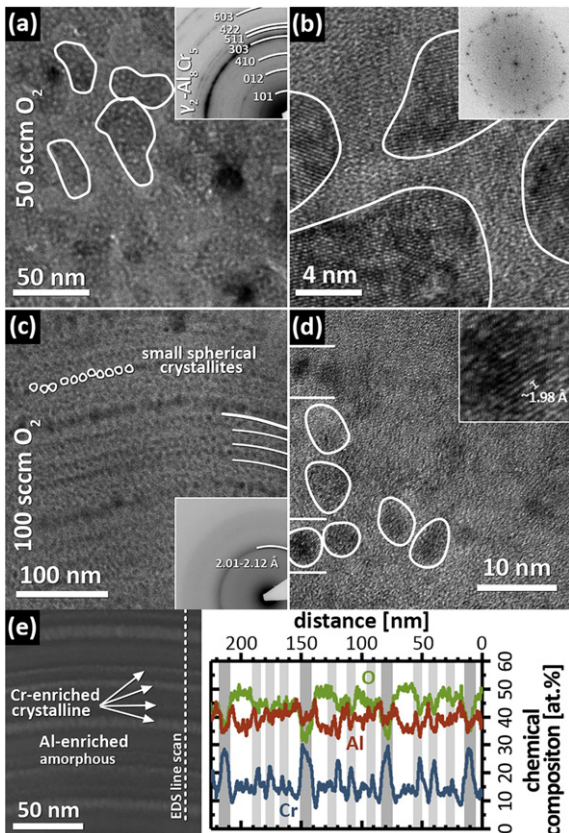


Fig. 1. TEM BF images of a substoichiometric $\text{Al}_{0.70}\text{Cr}_{0.30}$ -based coating prepared with 50 sccm O_2 p.a.s. with (a) lower and (b) higher magnification. The SAED inset in (a) and FFT inset in (b) indicate $\gamma_2\text{-Al}_8\text{Cr}_5$. Corresponding studies of $\text{Al}_{0.70}\text{Cr}_{0.30}$ -based coatings processed with 100 sccm O_2 p.a.s. are shown in (c) and (d). (e) STEM EDS study of the layered structure in (c). (For interpretation of the references to colour in this figure, the reader is referred to the web version of this article.)

Download English Version:

<https://daneshyari.com/en/article/5443443>

Download Persian Version:

<https://daneshyari.com/article/5443443>

[Daneshyari.com](https://daneshyari.com)